

Impact of Maleic Anhydride, Nanoclay, and Silica on Jute Fiber-reinforced Polyethylene Biocomposites

Md. Rezaur Rahman,^{a,*} Md. Mizanur Rahman,^b Sinin Hamdan,^b and Josephine Chang Hui Lai^a

Jute fiber/polyethylene biocomposites were prepared using a hot press molding technique. The effects of maleic anhydride, clay, and silica on the physical, mechanical, and thermal properties of jute fiber-reinforced polyethylene (PE) biocomposites with different fiber loadings (5, 10, 15, and 20 wt.%) were investigated. The biocomposites were characterized by Fourier transform infrared spectroscopy (FTIR), scanning electron microscopy (SEM), and thermogravimetric analysis (TGA). The mechanical properties were determined using a universal testing machine. The biocomposite specific surface area, pore volume, and pore size were investigated using the Brunauer-Emmett-Teller (BET) equation. Because of the Si-O-Si stretching vibration, the peak representing the O-H group significantly decreased in the range of 3200 to 3600 cm^{-1} . Jute fiber/PE Maleic anhydride silica composite (JFPEMASC) showed smoother surfaces, which indicated good distribution and better interfacial bonding between the fibers and matrix. The jute fiber/polyethylene/silica composites had a higher surface area and pore volume, with a lower pore size. JFPEMASC was more thermally stable than the other composites, with higher activation energy. JFPEMASC had the highest Young's modulus among all the biocomposites.

Keywords: Silica; Clay; Jute fiber; Mechanical properties; Surface morphology; BET

Contact information: a: Department of Chemical Engineering and Energy Sustainability and b: Department of Mechanical and Manufacturing Engineering, University Malaysia Sarawak, 94300 Kota Samarahan, Sarawak, Malaysia; *Corresponding author: reza_bawas@yahoo.com

INTRODUCTION

Natural fibers derived from annually renewable resources can be used as reinforcing fillers for composite materials. Natural fiber-reinforced composites have gained increased attention from researchers because of their advantages (Jahangir *et al.* 2012), including their renewable and environmentally friendly nature (Ali *et al.* 1994; Pankaj *et al.* 2013). Natural fiber-reinforced composites are used in the automotive, electronics, and engineering sectors (Baiardo *et al.* 2004). However, the use of natural fibers such as jute, sisal, flax, hemp, coir, wood, kenaf, cotton, and banana in bio-based composites has quickly expanded into construction materials (Ray *et al.* 2001). Natural fibers have some advantages such as abundant availability, low cost, low density, and sufficient mechanical properties compared with synthetic fibers (Mishra *et al.* 2003).

In recent years, the use of natural fibers as a reinforcement has gradually increased and is replacing the use of conventional inorganic fibers in polymer matrix composites. Among natural fibers, jute fiber is abundantly available for widespread cultivation in Asia (Elsayed *et al.* 2012). Moreover, jute fiber is inexpensive, lightweight, tough, and has good mechanical and thermal properties compared with other natural fibers such as sisal, flax,

hemp, cotton, and wood (Zaman *et al.* 2010). The conventional uses of jute fibers include floor coverings, packaging material, handicrafts, and textiles (Pankaj *et al.* 2013). However, the drawback of jute fiber is its hydrophilic nature, which is attributable to the presence of hemicellulose and cellulose molecules. Partially biodegradable polymers may be obtained from renewable resources, and they can be synthesized from petro-based chemicals or microbial-synthesized in the laboratory (Rahman *et al.* 2008).

Polyethylene (PE) is one of the most widely used polymers, both in developed and developing countries, and it has advantages economically and ecologically, as well as higher thermal stability (Rahman *et al.* 2010). Polyethylene (PE) possesses a variety of exceptional properties such as low density, high surface hardness, better abrasion resistance, good flex life, and exceptional electrical properties compared with other thermoplastics (Kabir *et al.* 2010). The hydrophilic nature of jute fiber and its hydrophobic polymer matrix create weak resistance to moisture absorption, and therefore contribute to the lower mechanical properties of jute fiber-reinforced composites (Saheb and Jog 1999; Mohanty *et al.* 2005). To overcome this problem, the PE matrix can be modified with maleic anhydride to enhance the hydrophobicity of PE. The hydrophobic PE helps to increase the fiber-matrix interaction which reflected on physical, mechanical, and thermal properties of PE biocomposites (Doan *et al.* 2007).

Polymer/clay biocomposites are a new class of materials that enhance the properties of lower filler loaded biocomposites compared with conventional filler composites (Garcia-Lopez *et al.* 2003). Clay is one of the best reinforcements for polymers because of its high characteristic ratio, but untreated clay is not easily incorporated into polymers because of its hydrophilicity (Liu *et al.* 2005). Modified nanoclay-reinforced polymer composites and their laminates enhance the physical, mechanical, and thermal properties of composites even at low filler quantities (Hossen *et al.* 2015).

SiO₂ particles are another significant reinforcement material for polymer composites (Kageyama *et al.* 1999; Kawashima *et al.* 2000; Wilder *et al.* 2003; Yu *et al.* 2005). Silica improves the elongation to the break point in polymer composites. Mark *et al.* (1997) reported enhanced mechanical, thermal, and optical properties after incorporating silica particles into the fiber and polymer matrix. The silica particle in the polymer matrix is vital in improving the properties of the composites (Lin *et al.* 2009).

The present work investigates the impact of maleic anhydride, clay, and silica on the physical, thermal, and mechanical properties of jute fiber-reinforced polyethylene biocomposites. The surface area, total pore volume, and adsorption pore radius of the biocomposites was also reported.

EXPERIMENTAL

Materials

The polyethylene used as the matrix material was manufactured by Siam Polyethylene Co., Ltd., Bangkok, Thailand. Maleic anhydride (C₄H₂O₃) was supplied by Marck Schuchardt OHG 85662 (Hohenbrunn, Germany). Nanoclay, Nanomer 1.30E, and montmorillonite clay surface modified with 25 to 30 wt. % octadecylamine was supplied by Sigma-Aldrich (St. Louis, MO, USA). Silicon dioxide (SiO₂; ~99%) was supplied by Sigma-Aldrich. Jute fibers were collected from the Bangladesh Jute Research Institute (BJRI), Dhaka, Bangladesh.

Composite Preparation

The middle parts of the jute fibers were chopped into 4 mm-long pieces. The chopped jute fibers were placed in an air convection oven for drying at 75 °C for 24 h. The fibers were mixed thoroughly with PE granules in different weight fractions based on fiber mass, and then maleic anhydride (MA), clay, and silica were added in a fixed weight fraction, as shown in Table 1. The mixture was placed in a mold and placed in a hot press for composite preparation at a temperature of 190 °C and under a pressure of 7 MPa.

Table 1. Different Weight Fractions (wt. %) of Jute Fiber/PE/MA/Clay/Silica for Biocomposite Preparation

Jute fiber (wt. %)	Jute fiber/PE composite (JFPEC)	Jute fiber/PE Maleic anhydride composite (JFPEMAC)		Jute fiber/PE Maleic anhydride clay composite (JFPEMACC)			Jute fiber/PE Maleic anhydride silica composite (JFPEMASC)		
	PE (wt. %)	PE (wt. %)	MA (wt. %)	PE (wt. %)	MA (wt. %)	Clay (wt. %)	PE (wt. %)	MA (wt. %)	Silica (wt. %)
5	95	93	2	91	2	2	92	2	1
10	90	88	2	86	2	2	87	2	1
15	85	83	2	81	2	2	82	2	1
20	80	78	2	76	2	2	77	2	1

Microstructural Analysis

Fourier transform infrared (FTIR) spectroscopy

The infrared spectra of the JFPEC, JFPEMAC, JFPEMACC, and JFPEMASC were recorded on a Shimadzu FT-IR 81001 Spectrophotometer (Kyoto, Japan). The obtained spectra are described in the Results and Discussion section. The transmittance range of the scan was 4000 to 500 cm⁻¹.

Scanning electron microscopy (SEM)

The fracture surfaces of the tensile specimens of the JFPEC, JFPEMAC, JFPEMACC, and JFPEMASC were examined using a Hitachi (TM 3030) supplied by JEOL (Tokyo, Japan) and a pitch emission scanning electron microscope (SEM). The SEM specimens were sputter-coated with gold prior to observation.

Adsorption isotherm

The nitrogen adsorption isotherms of JFPEC, JFPEMAC, JFPEMACC, and JFPEMASC were performed using a Quantachrome 4200e physicosorption analyzer (Florida, USA). The specimen (0.7368 g) was used at a constant machine temperature of 77 K under liquid nitrogen. The composites were degaussed at 350 °C in a vacuum for 1.5 h before the nitrogen adsorption isotherm was assembled. The specimen surface area and pore volume was analyzed using the Brunauer-Emmer-Teller (BET) equation, as follows,

$$S_{\text{BET}} = \frac{V_m \times A_{\text{CS}} \times N_o}{M} \quad (1)$$

where S_{BET} is specific surface area (m^2/g), V_m is the monolayer value (cm^3/g), A_{cs} is the settlement area of a molecule of nitrogen (m^2/mol), N_0 is Avogadro's number, and M is the molecular weight of nitrogen (g/mol).

Thermogravimetric analysis (TGA)

The thermal stability of specimens was examined using a Perkin Elmer thermal analyzer (Boston, USA). The specimen was heated from room temperature to $800\text{ }^\circ\text{C}$ at a heating rate of $10\text{ }^\circ\text{C}/\text{min}$ under N_2 using a flow rate of $30\text{ mL}/\text{min}$. The activation energy was calculated from TGA graphs based on the equation as follows:

$$\ln\left(\ln\frac{1}{y}\right) = \frac{E_a}{RT} + \text{constant} \quad (2)$$

Tensile test

Tensile tests were done according to ASTM D 638-01 (2002) using a Shimadzu MSC-5/500 universal testing machine (Kyoto, Japan) operating at a crosshead speed of $5\text{ mm}/\text{min}$. The specimen dimensions were $115\text{ mm (L)} \times 6.5\text{ mm (W)} \times 3.1\text{ mm (T)}$.

RESULTS AND DISCUSSION

Fourier Transform Infrared Spectroscopy

The FTIR spectra of JFPEC, JFPEMAC, JFPEMACC, and JFPEMASC at 15 wt.% fiber loadings are shown in Fig. 1. An absorption band in the region of 3600 to 3200 cm^{-1} is a characteristic stretching vibration of hydrogen bonds in O-H groups (Othman *et al.* 2006), and it was common to the JFPEC, JFPEMAC, and JFPEMACC spectra. The stretching vibration of O-H groups decreased because of the chemical modification by maleic anhydride with clay and silica. The absorption band of the C-H stretching vibration of methyl and methylene groups in cellulose and hemicelluloses showed its peak intensity at 2914 to 2846 cm^{-1} (Sinha and Rout 2008). The peaks at 1638 , 1648 , and 1646 cm^{-1} indicated the absorbed water in crystalline cellulose (Seki 2009), and the peak in the region at 1471 cm^{-1} reflected O-CH₃ stretching of the aromatic ring in lignin (Yang *et al.* 2007).

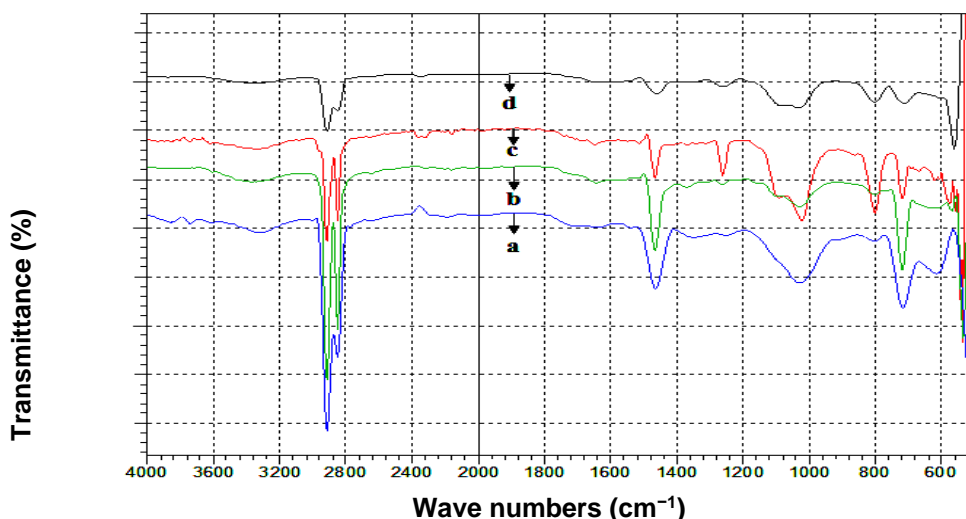


Fig. 1. FTIR spectra of a) JFPEC, b) JFPEMAC, c) JFPEMACC, and d) JFPEMASC

The peak intensity at 1265 cm^{-1} was assigned to the C-O stretching vibration of the acetyl group in lignin and hemicelluloses (Sinha and Rout 2008; Rosa *et al.* 2010). The absorption band of the Si-O-Si stretching vibration of JFPEMASC had their characteristic peaks at 1091 to 1028 cm^{-1} (Lai *et al.* 2015), whereas the absorption band at 802 cm^{-1} was related to the Si-O asymmetric stretching vibration (Wang *et al.* 2013). Because of the Si-O-Si stretching vibration, the peak representing the O-H group significantly decreased from 3600 to 3200 cm^{-1} . The silica replaced the hydrogen atom in OH groups to produce Si-O-Si stretching vibration that reduced the OH group's intensity (Sadek *et al.* 2013). This decreased the C-H stretching vibration, O-CH₃ stretching, and C-O stretching vibration. The JFPEMACC had a peak region at 1089 to 1020 cm^{-1} for C-H deformation on the alkyl groups bond, whereas the absorption band occurred at 1026 cm^{-1} for the C-O stretching vibration of the JFPEC and JFPEMAC, which belonged to polysaccharides in cellulose (Liu *et al.* 2009; Atuanya and Ibhadoode 2011; Deka and Maji 2013). However, JFPEMASC showed Si-O-Si stretching vibration, as confirmed by peaks at 1091 and 1028 cm^{-1} (Fig. 1(d)).

Scanning Electron Microscopy

The interfacial bonding between the jute fiber, PE matrix modified by maleic anhydride, clay, and silica nano filler were investigated by SEM (Fig. 2). There was a significant difference in the interface interaction of jute fiber, modified PE matrix with clay, and jute fiber, modified PE matrix with nanosilica in the composite system. As shown in Figs. 2(a) and (b), there were uneven surfaces, pullout traces of fiber with void spaces, and agglomeration in the composites (Hossain *et al.* 2011; Islam *et al.* 2011). The images indicated that there was weak interface bonding and poor distribution between the fibers and matrix. In addition, Fig. 2(c) shows good interface bonding and a lower number of pullout traces of fiber. Moreover, Fig. 2(d) shows a smoother surface and lower agglomeration compared with Figs. 2(a), (b), and (c), respectively. Figure 2(d) indicates that there was good distribution and better interfacial bonding between the fibers and matrix. The strong interfacial bonding between the fiber and PE matrix was caused by the surface modification of jute fiber with maleic anhydride and silica particles (Bikiaris *et al.* 2005; Ahmed *et al.* 2014).

The silica particles were integrated into the jute fiber and matrix to reduce the agglomeration and increased surface morphology of the composite, as shown in Fig. 2(d). Figure 2(d) clearly shows that silica improved the morphological properties compared with Figs. 2(a), (b), and (c). Enhanced morphological properties were also reflected in the mechanical and thermal properties of the composites (discussed below).

Adsorption Isotherm

The nitrogen adsorption isotherms of JFPEC, JFPEMAC, JFPEMACC, and JFPEMASC are shown in Fig. 3. The specific surface areas were measured based on N₂ sorption at 77 K, using the Brunauer-Emmer-Teller (BET) model (Lowell *et al.* 2004). The specific surface areas of JFPEC, JFPEMAC, JFPEMACC, and JFPEMASC were 3.184, 5.770, 6.983, and 9.268 m²/g, respectively, which indicates an enhanced surface area of JFPEMASC compared with the other specimens. Because of the good distribution of clay and silica in the composites, they enhanced the compatibility between the fiber and matrices. The enhanced compatibility decreased the surface void and improved their accessibility for nitrogen adsorption.

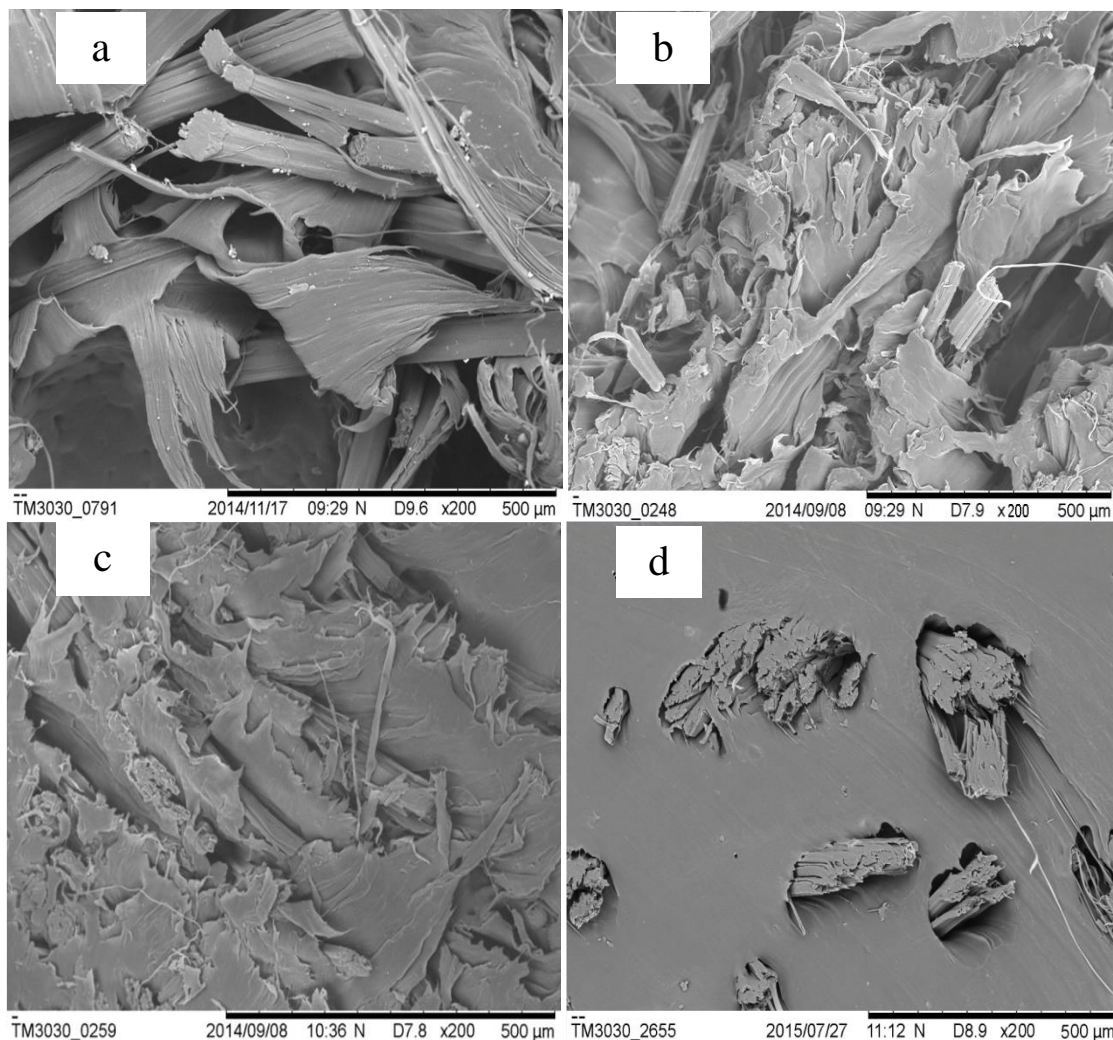


Fig. 2. SEM images of the fracture surfaces of a) JFPEC, b) JFPEMAC, c) JFPEMACC, and d) JFPEMASC

The specific surface area and total pore volume of composites significantly increased, whereas the adsorption pore radius decreased (Table 2). The isotherm patterns showed the presence of a hysteresis loop, the characteristic feature of the type IV isotherms according to the original IUPAC classification (Sing *et al.* 1985; Kaneko 1994). The adsorption isotherms indicate that the pores were mesopores (> 2 nm but < 50 nm) (Sing *et al.* 1985; Leofanti *et al.* 1998).

The N_2 adsorption isotherm initially had an increasing section up to $P/P_0 = 0.20$, and after that, it showed a slightly straight section, ranging up to $P/P_0 = 0.40$. Finally, the isotherm exhibited an enhanced sweep slightly near the saturation pressure. A comparable pattern of isotherm was observed for JFPEC, JFPEMAC, JFPEMACC, and JFPEMASC, with the initial rising section extending up to $P/P_0 = 0.40$, 0.40 , 0.40 , and 0.30 , respectively. The improvement in the N_2 adsorption at optimal P/P_0 values was observed for JFPEMASC. This could be caused by the effect of maleic anhydride and silica on the composite system, maximizing the specific surface area and average pore volume with lesser pore size, as reflected in the SEM images.

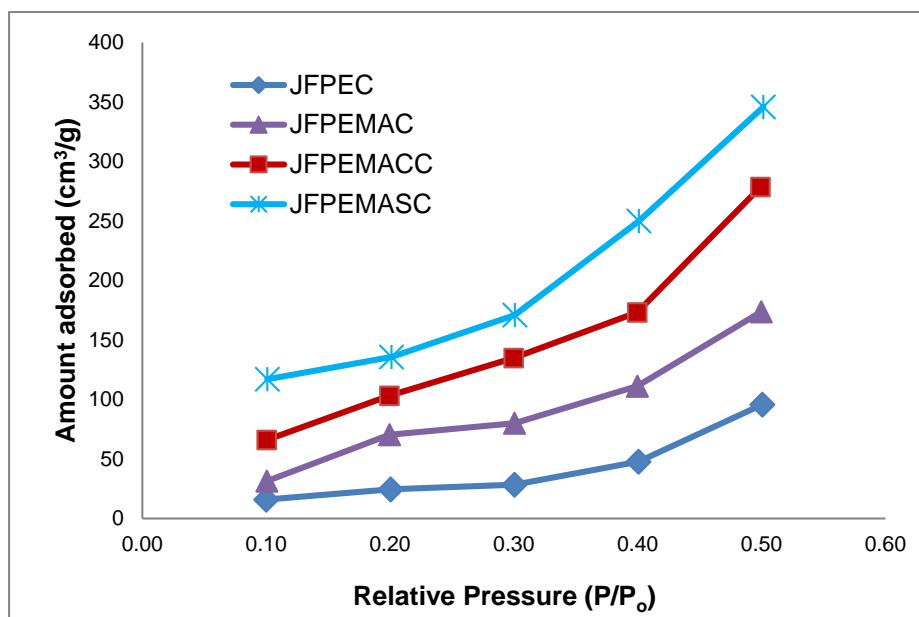


Fig. 3. Nitrogen adsorption isotherms of JFPEC, JFPEMAC, JFPEMACC, and JFPEMASC

Table 2. Specific Surface Area, Total Pore Volume, Adsorption Pore Radius, and Type of Isotherms for JFPEC, JFPEMAC, JFPEMACC, and JFPEMASC

Sample Names	Specific Surface Area (m ² /g)	Total Pore Volume (cc/g)	Adsorption Pore Radius (nm)	Type of Isotherms
JFPEC	3.2	1.7	2.3	IV
JFPEMAC	5.8	3.7	1.7	IV
JFPEMACC	7.0	4.9	1.8	IV
JFPEMASC	9.3	7.4	1.6	IV

Thermogravimetric Analysis (TGA)

The thermal stabilities of JFPEC, JFPEMAC, JFPEMACC, and JFPEMASC are shown in Fig. 4. The thermal stability of JFPEMASC significantly increased compared with JFPEC, JFPEMAC, and JFPEMACC. There were three stages of weight loss for the composites; the first stage of weight loss occurred at temperatures lower than 200 °C, which corresponded to the dehydration of the moisture content. The second stage of weight loss occurred between 200 and 310 °C, which corresponded to the degradation of cellulose and hemicellulose (Chen *et al.* 2015). The third stage of weight loss occurred above 380 °C, which represents lignin and polymer degradation (Kabir *et al.* 2013; Chen *et al.* 2015). The weight loss of JFPEC, JFPEMAC, JFPEMACC, and JFPEMASC were 7.13%, 4.52%, 4.43%, and 2.91%, respectively. There was no degradation up to 160 °C, and the initial decomposition started at 323, 343, 360, and 381 for JFPEC, JFPEMAC, JFPEMACC, and JFPEMASC, respectively (Islam *et al.* 2011). The final decomposition (T_f) of JFPEMASC was higher than of JFPEC, JFPEMAC, and JFPEMACC (Table 3). The bonding compatibility of JFPEMASC was higher than that of JFPEC, JFPEMAC, and JFPEMACC because of the important role of clay and silica in the composite system, which is discussed in the SEM results.

The TGA curve showed that JFPEMASC was more thermally stable than the other composites. The activation energy of JFPEMASC was significantly higher than that of JFPEC, JFPEMAC, and JFPEMACC. Higher activation energy showed higher stability of the composites.

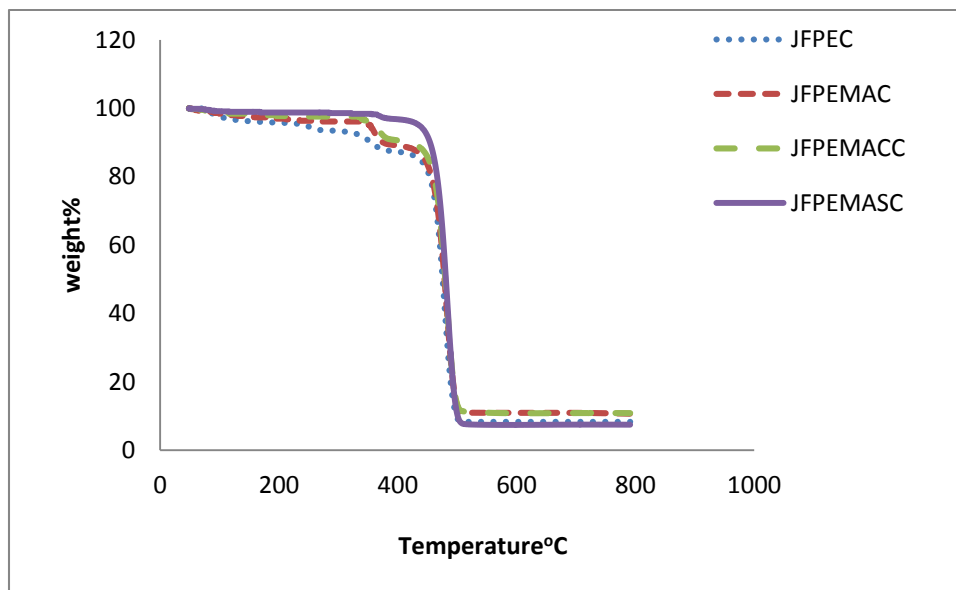


Fig. 4. TGA curves of JFPEC, JFPEMAC, JFPEMACC, and JFPEMASC

Table 3. Thermal Characteristics of JFPEC, JFPEMAC, JFPEMACC, and JFPEMASC

Name of the samples	T_i (°C) ^a	T_m (°C) ^b	T_f (°C) ^c	W_{Ti} (%) ^d	W_{Tm} (%) ^e	W_{Tf} (%) ^f	Activation energy, E_a (KJ/mol)
JFPEC	323	454	502	92.87	79.43	8.52	223.08
JFPEMAC	343	447	506	95.48	84.12	11.18	242.95
JFPEMACC	360	443	517	95.57	87.50	11.23	246.99
JFPEMASC	381	438	532	97.09	94.54	7.49	310.28

^a Temperature corresponding to the beginning of decomposition

^b Temperature corresponding to the maximum rate of mass loss

^c Temperature corresponding to the end of decomposition

^d Mass loss corresponding to the beginning of decomposition

^e Mass loss corresponding to the maximum rate of mass loss

^f Mass loss corresponding to the end of decomposition

Tensile Properties

The tensile strength and Young's modulus of the different fiber loadings for JFPEC, JFPEMAC, JFPEMACC, and JFPEMASC are shown in Fig. 5. The tensile strength and Young's modulus gradually increased up to a 15% fiber loading and then decreased for all composites with higher fiber loadings. This result reflects the weak interfacial bonding, lower compatibility, and higher agglomeration between the fiber and matrices. The composition at 15 wt.% jute fiber was the best of those tested. Among the composites, JFPEMASC showed the maximum tensile strength compared with JFPEC, JFPEMAC, and

JFPEMACC. The tensile strength increased significantly when silica and maleic anhydride were added to the fiber and PE matrix. Clay and silica improved the interfacial bonding between the fiber and PE matrix because of the surface modification of PE matrix with maleic anhydride that reduced the void spaces (Bikiaris *et al.* 2005). Jute fiber-reinforced polyethylene biocomposites showed better tensile strength compared to treated jute composites with tensile strength of 17 MPa (Patel *et al.* 2008). For tensile modulus, jute fiber-reinforced polyethylene biocomposites showed higher values compared to treated fiber biocomposites with 0.9 GPa (Saravana Bavan and Mohan Kumar 2014).

However, JFPEMASC had the highest Young's modulus, followed by JFPEC, JFPEMAC, and JFPEMACC. This result was due to higher compatibility between the fiber and matrix in the composite system; silica acted as a reinforcement in the fiber and matrix. The agglomeration of fiber-matrix interaction increased the rate of decreased in tensile strength and Young's modulus in higher fiber loading (20wt.%) (Deshmukh *et al.* 2010).

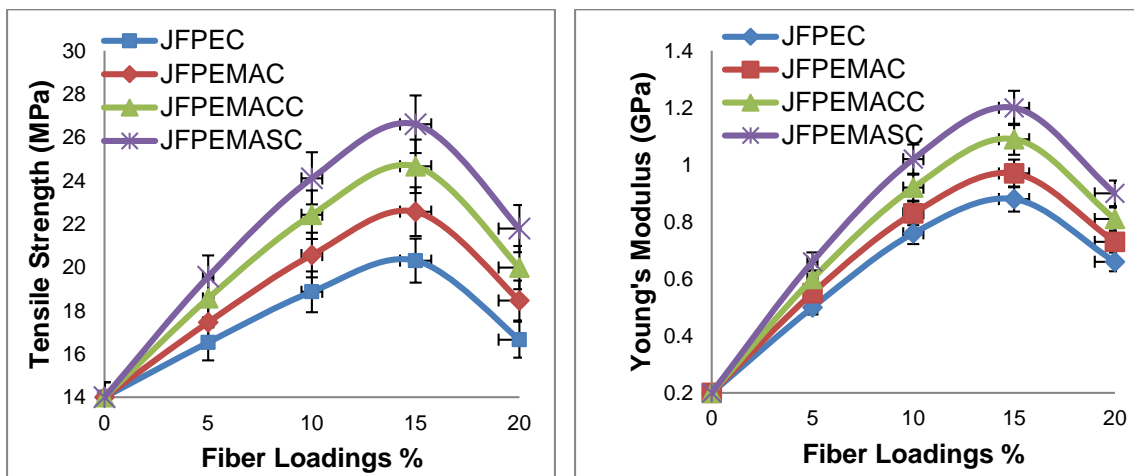


Fig. 5. Variation of tensile strengths and Young's modulus at different fiber loadings for JFPEC, JFPEMAC, JFPEMACC, and JFPEMASC

CONCLUSIONS

1. Jute fiber/polyethylene biocomposites were prepared using a hot press molding technique, and the physical, mechanical, and thermal properties of biocomposites with different fiber loadings (5, 10, 15, and 20 wt.%) were examined.
2. The stretching vibration of O-H groups in treated biocomposites decreased due to the chemical modification by maleic anhydride with clay and silica compared to the untreated composites.
3. The SEM images of the treated biocomposites showed that the fiber and matrix interaction was stronger compared to untreated one. This was due to the incorporation of silica particles into the jute fiber and matrix that reduced the agglomeration and improved the surface morphology of the biocomposite.
4. JFPEMASC showed the highest specific surface area and average pore volume with lower pore size followed by JFPEC, JFPEMAC, and JFPEMACC.

5. The bonding compatibility of JFPEMASC was higher than that of JFPEC, JFPEMAC, and JFPEMACC which improved the thermal stability of the treated biocomposites.
6. The incorporation of clay and silica improved the tensile strength and modulus of the treated biocomposites due to the strong interfacial bonding between the fiber and PE matrix.
7. This biocomposites can be applied in interior and exterior usage as well as used as construction materials.

ACKNOWLEDGMENTS

The authors are grateful for support from the University of Malaysia at Sarawak, Grant. No. UNIMAS/CoERE/Grant/2014/06.

REFERENCES CITED

- Ahmed, A. S., Islam, M. S., Hassan, A., Haafiz, M. K. M., Islam K. N., and Arjmandi, R. (2014). "Impact of succinic anhydride on the properties of jute fiber/polypropylene biocomposites," *Fib. Polym.* 15(2), 307. DOI: 10.1007/s12221-014-0307-8
- Ali, K. M. I., Khan, M. A., and Husain, M. M. (1994). "Role of additives in wood plastic composite of water soluble monomer," *Radiat. Phys. Chem.* 44(4), 421-425. DOI: 10.1016/0969-806X(94)90082-5
- ASTM D 638-01. (2002). "Standard test methods for tensile properties of plastics," ASTM International, West Conshohocken, PA, USA.
- Atuanya, C. U., and Ibhado, A. O. A. (2011). "Characterization of Okhuen (*Brachystegia nigerica*) wood as a potential reinforcement for polymer composites," *Int. J. Eng. Technol.* 11(4), 52-59.
- Baiardo, M., Zini, E., and Scandola, M. (2004). "Flax fibre-polyester composites," *Compos. Part A* 35(6), 703-710. DOI: 10.1016/j.compositesa.2004.02.004
- Bikiaris, D. N., Vassiliou, A., Pavlidou, E., and Karayannidis, G. P. (2005). "Compatibilisation effect of PP-g-MA copolymer on iPP/SiO₂ nanocomposites prepared by melt mixing," *Eur. Polym. J.* 41(9), 1965-1978. DOI: 10.1016/j.eurpolymj.2005.03.008
- Chen, R. S., Ab Gani, M. H., Ahmad, S., Salleh, M. N., and Tarawneh, M. A. (2015), "Rice husk flour biocomposites based on recycled high-density polyethylene/polyethylene terephthalate blend: Effect of high filler loading on physical, mechanical and thermal properties," *J. Compos. Mater.* 49(10), 1241. DOI: 10.1177/0021998314533361
- Deka, B. K., and Maji, T. K. (2013). "Effect of SiO₂ and nanoclay on the properties of wood polymer nanocomposite," *Polym. Bull.* 70(2), 403. DOI: 10.1007/s00289-012-0799-6
- Deshmukh, S. P., Rao, A. C., Gaval, V. R., Joseph, S., and Mahanwar, P. A. (2010). "Effect of particle size and concentration on mechanical and electrical properties of the mica filled PVC," *J. Miner. Mater. Charact. Eng.* 9(9), 831. DOI: 10.1177/0892705710393114

- Doan, T. T. L., Brodowsky, H., and Mader, E. (2007). "Jute fibre/polypropylene composites II. Thermal, hydrothermal and dynamic mechanical behavior," *Compos. Sci. Technol.* 67, 2707-2714. DOI: 10.1016/j.compscitech.2007.02.011
- Elsayed, A. E., Mohamed, S., Hassan, A., and Hamada, H. (2012). "Mechanical properties of natural jute fabric/jute mat fiber reinforced polymer matrix hybrid composites," *Adv. in Mech. Eng.* 2012, 12.
- Garcia-Lopez, D., Picazo, O., Merino, J. C., and Pastor, J. M. (2003). "Polypropylene-clay nanocomposites: Effect of compatibilizing agents on clay dispersion," *Eur. Polym. J.* 39(5), 945-950. DOI: 10.1016/s0014-3057(02)00333-6
- Hossain, M. K., Dewan, M. W., Hosur, M., and Jeelani, S. (2011). "Mechanical performances of surface modified jute fiber reinforced biopol nanophased green composites," *Compos. Part B* 42(6), 1701-1707. DOI: 10.1016/j.compositesb.2011.03.010
- Hossen, M. F., Hamdan, S., Rahman, M. R., Rahman, M. M., Liew, F. K., and Lai, J. C. H. (2015). "Effect of fiber treatment and nanoclay on the tensile properties of jute fiber reinforced polyethylene/clay nanocomposites," *Fib. Polym.* 16(3), 479-485. DOI: 10.1007/s12221-015-0479-x
- Islam, M. S., Hamdan, S., Rahman, M. R., Jusoh, I., Ahmad, A. S., and Idrus, M. (2011). "Dynamic Young's modulus, morphological, and thermal stability of 5 tropical light hardwoods modified by benzene diazonium salt treatment," *BioResources* 6, 737-750. DOI: 10.15376/biores.6.1.737-750
- Jahangir, A. K., Khan, M. A., and Islam, R. (2012). "Effect of mercerization on mechanical, thermal and degradation characteristics of jute fabric-reinforced polypropylene composites," *Fib. Polym.* 13(10), 1300-1309. DOI: 10.1007/s12221-012-1300-8
- Kabir, M. A., Huque, M. M., Islam, M. R., and Bledzki, A. K. (2010). "Mechanical properties of jute fiber reinforced polypropylene composite: Effect of chemical treatment by benzenediazonium salt in alkaline medium," *BioResources* 5(3), 1618-1625. DOI: 10.15376/biores.5.3.1618-1625
- Kabir, M. M., Islam, M. M., and Wang, H. (2013). "Mechanical and thermal properties of jute fibre reinforced composites," *J. Multifunc. Compos.* 1(1), 71-77. DOI: 10.12783/issn.2168-4286/1.1/Islam
- Kageyama, K., Tamazawa, J., and Aida, T. (1999). "Extrusion polymerization: Catalyzed synthesis of crystalline linear polyethylene nanofibers within a mesoporous silica," *Sci.* 285(5436), 2113-2115. DOI: 10.1126/science.285.5436.2113
- Kaneko, K. (1994). "Determination of pore size and pore size distribution: 1. Adsorbents and catalysts," *J. Membr. Sci.* 96(1-2), 59-89. DOI: 10.1016/0376-7388(94)00126-x
- Kawashima, D., Aihara, T., Kobayashi, Y., Kyotani, T., and Tomita, A. (2000). "Preparation of mesoporous carbon from organic polymer/silica nanocomposites," *Chem. Mater.* 12(1), 3397-3401. DOI: 10.1021/cm0004351
- Lai, J. C. H., Rahman, M. R., Hamdan, S., Liew, F. K., Rahman, M. M., and Hossen, M. F. (2015). "Impact of nanoclay on physicomechanical and thermal analysis of polyvinyl alcohol/fumed silica/clay nanocomposites," *J. Appl. Polym. Sci.* 132(15). DOI: 10.1002/APP.41843
- Leofanti, G., Padovan, M., Tozzola, G., and Venturelli, B. (1998). "Surface area and pore texture of catalysts," *Catalysis Today* 41(1-3), 207-219. DOI: 10.1016/S0920-5861(98)00050-9

- Lin, O. H., Ishak, Z. A. M., and Akil, H. M. (2009). "Preparation and properties of nanosilica-filled polypropylene composites with PP-methyl POSS as compatibiliser," *Mater. Des.* 30(3), 748-751. DOI: 10.1016/j.matdes.2008.05.007
- Liu, D., Han, G., Huang, J., and Zhang, Y. (2009). "Composition and structure study of natural *Nelumbo nucifera* fiber," *Carbo. Polym.* 75(1), 39-43. DOI: 10.1016/j.carbpol.2008.06.003
- Liu, W., Hoa, S. V., and Pugh, M. (2005). "Organoclay-modified high performance epoxy nanocomposites," *Compos. Sci. Technol.* 65(2), 307-316. DOI: 10.1016/j.compscitech.2004.07.012
- Lowell, S., Shields, J. E., Thomas, M. A., and Thommes, M. (2004). *Characterization of Porous Solids and Powders: Surface Area, Pore Size and Density*, Kluwer Academic Publishers, Dordrecht, The Netherlands.
- Mark, J. E., Pu, Z., Jethmalani, J. M., and Ford, W. T. (1997). "Effects of aggregation and aggregation of silica in the reinforcement of poly(methyl acrylate) elastomers," *Chem. Mater.* 9, 2442-2447. DOI: 10.1021/cm970210j
- Mishra, S., Mohanty, A. K., Drzal, L. T., Misra, M., Parija, S., Nayak, S. K., and Tripathy, S. S. (2003). "Studies on mechanical performance of biofibre/glass reinforced polyester hybrid composites," *Compos. Sci. Technol.* 63(10), 1377-1385. DOI: 10.1016/S0266-3538(03)00084-8
- Mohanty, A. K., Misra, M., and Drzal, L. T. (2005). *Natural Fibers, Biopolymers, and Biocomposites*, Taylor & Francis, New York, NY, USA.
- Othman, N., Ismail, H., and Mariatti, M. (2006). "Effect of compatibilisers on mechanical and thermal properties of bentonite filled polypropylene composites," *Polym. Degrad. Stabil.* 91(8), 1761-1774. DOI: 10.1016/j.polymdegradstab.2005.11.022
- Pankaj, K. A., Raghu, N., Karmarkar, A., and Chuahan, S. (2013). "Jute-polypropylene composites using m-TMI-grafted-polypropylene as a coupling agent," *Mater. Des.* 43, 112-117. DOI: 10.1016/j.matdes.2012.06.026
- Ray, D., Sarkar, B. K., Rana, A. K., and Bose, N. R. (2001). "The mechanical properties of vinylester resin matrix composites reinforced with alkali-treated jute fibers," *Compos. Part A* 32(1), 119-127. DOI: 10.1016/S1359-835X(00)00101-9
- Rahman, M. R., Huque, M. M., Islam, M. N., and Hasan, M. (2008). "Improvement of physico-mechanical properties of jute fiber reinforced polypropylene composites by post-treatment," *Compos. Part A* 39(11), 1739-1747. DOI: 10.1016/j.compositesa.2008.08.002
- Rahman, M. R., Hasan, M., Huque, M. M., and Islam, M. N. (2010). "Physico-mechanical properties of jute fiber reinforced polypropylene composites," *J. Reinf. Plast. Compos.* 29(3), 445-455. DOI: 10.1177/0731684408098008
- Rosa, I. M. D., Kenny, J. M. D. P., and Sarasini, C. S. F. (2010). "Morphological, thermal and mechanical characterization of okra (*Abelmoschus esculentus*) fibres as potential reinforcement in polymer composites," *Compos. Sci. Technol.* 70(1), 116-122. DOI: 10.1016/j.compscitech.2009.09.013
- Sadek, O. M., Reda, S. M., and Al-Bilali, R. K. (2013). "Preparation and characterization of silica and clay-silica core-shell nanoparticles using sol-gel method," *Adv. in Nanopart.* 2(2), 165-175. DOI: 10.4236/anp.2013.22025
- Saheb, D. N., and Jog, J. P. (1999). "Natural fiber polymer composites: A review," *Adv. Polym. Technol.* 18(4), 351-353. DOI: 10.1002/(SICI)1098-2329(199924)18:4<351::AID-ADV6>3.0.CO;2-X

- Seki, Y. (2009). "Innovative multifunctional siloxane treatment of jute fiber surface and its effect on the mechanical properties of jute/thermoset composites," *Mater. Sci. Eng. A*, 508(1–2), 247-252. DOI: 10.1016/j.msea.2009.01.043
- Sing, K. S. W., Everett, D. H., Haul, R. A. W., Moscou, L., Pierotti, R. A., Rouquero, J., and Siemieniewska, T. (1985). "Physical and biophysical chemistry division commission on colloid and surface chemistry including catalysis," *Pure. Appl. Chem.* 57(4), 603-619.
- Sinha, E., and Rout, S. K. (2008). "Influence of fibre-surface treatment on structural, thermal and mechanical properties of jute," *J. Mater. Sci.* 43(8), 2590-2601. DOI: 10.1007/s10853-008-2478-4
- Wang, X., Wang, L., Su, Q., and Zheng, J. (2013). "Use of unmodified SiO₂ as nanofiller to improve mechanical properties of polymer-based nanocomposites," *Compos. Sci. Technol.* 89, 52-60. DOI: 10.1016/j.compscitech.2013.09.018
- Wilder, E. A., Braunfeld, M. B., Jinnai, H., Hall, C. K., Agard, D. A., and Spontak, R. J. (2003). "The molecular structure and intermolecular interactions of 1,3:2,4-dibenzylidene-D-sorbitol," *Mol. Phys.* 101(19), 3017-3027. DOI: 10.1080/00268970310001597327
- Yang, H., Yan, R., Chen, H., Lee, D. H., and Zheng, C. (2007). "Characteristics of hemicellulose, cellulose and lignin pyrolysis," *Fuel* 86(12–13), 1781-1788. DOI: 10.1016/j.fuel.2006.12.013
- Yu, T., Lin, J., Xu, J., and Ding, W. (2005). "Nanocomposites of vinyl chloride-acrylonitrile copolymer and silica," *J. Polym. Sci. Part B: Polym. Phys.* 43(21), 3127-3134. DOI: 10.1002/polb.20606
- Zaman, H. U., Khan, A., Khan, R. A., Huq, T., Khan, M. A., Shahruzzaman, M., Rahman, M. M., Al-Mamun, M., and Poddar, P. (2010). "Preparation and characterization of jute fiber fabrics reinforced urethane based thermoset composites: Effect of UV radiation," *Fib. Polym.* 11(2), 258-265. DOI: 10.1007/s12221-010-0258-7

Article submitted: March 14, 2016; Peer review completed: April 23, 2016; Revised version received and accepted: May 9, 2016; Published: May 16, 2016.
DOI: 10.15376/biores.11.3.5905-5917